

The implication from these comparisons is that there is appreciable metal character in the unpaired electron density. Some radical character is implied indirectly from the limited chemical stability of the cobalt(I) species, since such species are likely to undergo irreversible chemical reactions with solvent.<sup>19,21,22</sup> The ability to delocalize some electron density onto the thioether donors is also likely to be the key to the different redox chemistry between  $\text{CoN}_6$  and  $\text{CoN}_3\text{S}_3$  macrobicyclic complexes.

**Acknowledgment.** We thank Dr. M. Gunter for assistance in recording the ESR spectrum at liquid-helium temperature.

**Registry No.** II, 81505-65-9; IIIa, 81505-68-2; IIIb, 92490-30-7; IV, 81600-15-9;  $\text{Co}(\text{ten})^{2+}$ , 92490-31-8;  $\text{Co}(\text{ten})$ , 92524-60-2;  $\text{Co}(\text{azacapten})^{2+}$ , 86161-69-5;  $\text{Co}(\text{azacapten})^+$ , 92490-36-3;  $\text{Co}((\text{NH}_3^+)\text{capten})^{3+}$ , 92490-34-1;  $\text{Co}((\text{NH}_3^+)\text{capten})^{2+}$ , 92490-35-2;  $\text{Co}((\text{NO}_2)\text{capten})^{2+}$ , 92490-32-9;  $\text{Co}((\text{NO}_2)\text{capten})^+$ , 92490-33-0;  $\text{Co}((\text{NO})\text{capten})^{3+}$ , 92490-37-4;  $\text{Co}((\text{NHOH})\text{capten})^{3+}$ , 92490-38-5;  $\text{NaClO}_4$ , 7601-89-0;  $\text{Me}_4\text{NOSO}_2\text{CF}_3$ , 25628-09-5.

## Notes

Contribution from the Department of Chemistry, Technion—Israel Institute of Technology, Haifa 32000, Israel, and Institute of Inorganic Chemistry, University of Frankfurt, D-6000 Frankfurt, West Germany

### On the Nonobservability of Cubic $\text{P}_8$

E. Amitai Halevi,<sup>1a</sup> Hans Bock,<sup>\*1b</sup> and Bernhard Roth<sup>1b</sup>

Received January 20, 1984

One of the more perplexing features of the chemistry of elemental phosphorus is the absence of any  $\text{P}_6$  or  $\text{P}_8$  species from the manifold of its allotropic forms.<sup>2</sup> This point has been underscored in a recent photoelectron spectroscopic investigation of the equilibrium  $\text{P}_4 \rightleftharpoons 2\text{P}_2$ .<sup>3</sup> No other species was detected in the vapor phase up to 1470 K. Specifically,  $\text{P}_8$ , the expected product of the dimerization of  $\text{P}_4$ , and  $\text{P}_6$ , which might be formed by the addition of  $\text{P}_2$  to  $\text{P}_4$ , were conspicuously absent.

Exploratory semiempirical computations, using MNDO,<sup>4</sup> disclosed a number of  $\text{P}_6$  and  $\text{P}_8$  species, each at a minimum in the potential energy surface; several of them are calculated to be thermodynamically more stable than their dissociation products. The failure to observe any particular one of them could arise from either of two causes: (1) An insurmountable kinetic barrier prevents its formation. (2) Although it may be formed with relative ease, it is immediately converted to some more stable species; in the present instance, this would presumably be  $(\text{P}_4)_n$ , i.e. common red phosphorus.

In this paper we consider the most stable of these molecules, cubic ( $O_h$ )  $\text{P}_8$ . Possible pathways leading to other  $\text{P}_8$  and  $\text{P}_6$  species are presently being explored.

### Ground-State Energies and Geometries

The calculated energies and geometries of  $\text{P}_2$ ,  $\text{P}_4$ , and  $\text{P}_8$  are summarized in Table I.

The reliability of the computational method is confirmed by the good agreement of the value ( $\Delta H^\circ = 43$  kcal/mol) calculated for the equilibrium  $\text{P}_4 \rightleftharpoons 2\text{P}_2$ . The temperature dependence of the equilibrium constant yields  $\Delta H^\circ = 55$  kcal/mol over the range 1170–1470 K,<sup>3</sup> whereas the best thermochemical value in this temperature range is  $53 \pm 1$  kcal/mol.<sup>5</sup>

The value ( $\Delta H^\circ = -68$  kcal/mol), calculated for the equilibrium  $2\text{P}_4 \rightleftharpoons \text{P}_8$ , leaves no doubt that cubic  $\text{P}_8$  is substantially more stable than two tetrahedral  $\text{P}_4$  molecules, as simple considerations of steric strain would suggest. Our

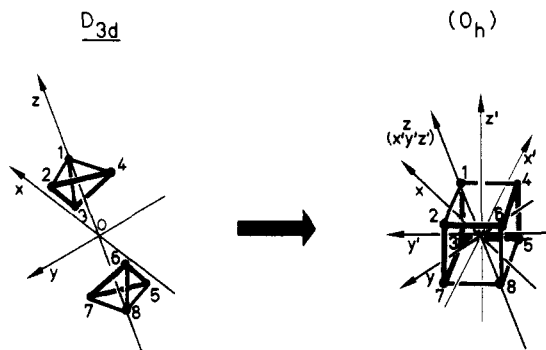


**Figure 1.** Highest symmetry reaction path ( $D_{3d}$ ) for dimerization of tetrahedral  $\text{P}_4$  to cubic  $\text{P}_8$ . Bonds broken: (23), (34), (42), (56), (67), (75). Bonds made: (26), (64), (45), (53), (37), (72).

**Table I.** Calculated Enthalpies of Formation and Bond Lengths of Various Species of Elemental Phosphorus

species	symmetry	$\Delta H_f^\circ$ , kcal	$r_{\text{PP}}$ , Å	
			calcd	exptl
$\text{P}_2$	$D_{\infty h}$	40.7	1.693	1.894
$\text{P}_4$	$T_d$	36.2	2.052	2.21
$\text{P}_8$	$O_h$	4.1	2.074	

results are confirmed to some extent by Trinquier, Malrieu, and Daudey,<sup>6</sup> who performed ab initio pseudopotential SCF calculations employing double $\zeta$  basis sets and found (without inclusion of d polarization functions) cubic  $\text{P}_8$  to be more stable than two  $\text{P}_4$  by 10 kcal/mol. They are in conflict with those of Fluck, Pavlidou, and Janoschek,<sup>7</sup> who find  $\text{P}_8$  to be unstable with respect to two  $\text{P}_4$  molecules by some 47 kcal/mol. These authors did not optimize the P–P distance for  $\text{P}_8$  but used the experimental value in  $\text{P}_4$  for both molecules. It is clear from the table that, although bond lengths calculated by MNDO are consistently shorter than the experimental ones, the P–P bond is appreciably longer in  $\text{P}_8$  than in  $\text{P}_4$ . It follows that the energy calculated for the former at the experimental bond length of the latter is necessarily too high.

### Qualitative Symmetry Analysis (OCAMS)

The cubic  $\text{P}_8$  molecule has  $O_h$  symmetry. If it is stretched along one of its diagonals, its symmetry is reduced to  $D_{3d}$ . Further elongation of the diagonal, with retention of  $D_{3d}$  symmetry, eventually produces two  $\text{P}_4$  molecules, so orbital correspondence analysis in maximum symmetry (OCAMS)<sup>8</sup> is carried out in  $D_{3d}$ , the highest symmetry compatible with

(1) (a) Technion—Israel Institute of Technology. (b) University of Frankfurt.  
 (2) See, e.g., Figure 8 of: Corbridge, D. E. C. "The Structural Chemistry of Phosphorus"; Elsevier: Amsterdam, 1974; p 22.  
 (3) Bock, H.; Müller, H. *Inorg. Chem.*, companion article in this issue.  
 (4) Dewar, M. J. S.; Thiel, W. *J. Am. Chem. Soc.* **1977**, *99*, 4899, 4907.  
 (5) "JANAF Thermochemical Tables"; Dow: Midland, MI 1960.

(6) Trinquier, G.; Malrieu, J.-P.; Daudey, J.-P. *Chem. Phys. Lett.* **1981**, *80*, 552.  
 (7) Fluck, E.; Pavlidou, C. M. E.; Janoschek, R. *Phosphorus Sulfur* **1979**, *6*, 469.  
 (8) (a) Halevi, E. A. *Helv. Chim. Acta* **1975**, *58*, 2136. (b) Katriel, J.; Halevi, E. A. *Theor. Chim. Acta* **1975**, *40*, 1.

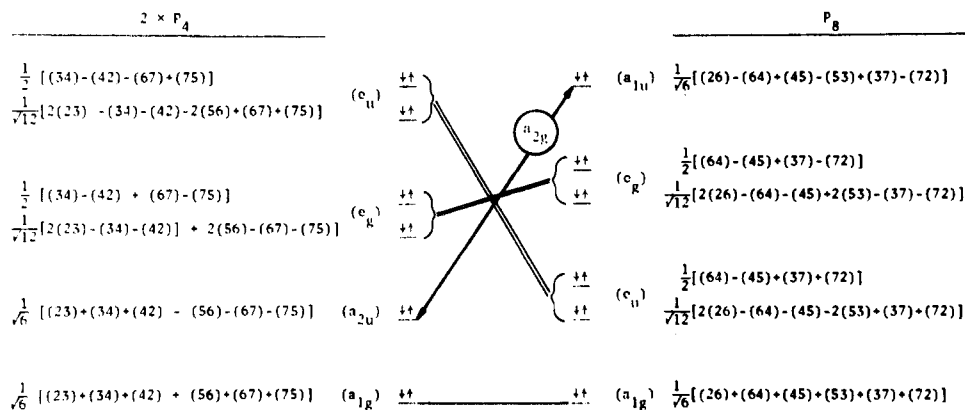


Figure 2. Correspondence diagram for dimerization of  $P_4$  in  $D_{3d}$ . The localized bond orbitals are as indicated in Figure 1.

the fragmentation of  $P_8$  to two  $P_4$  units. The reverse reaction, the dimerization of two  $P_4$  tetrahedra in the staggered face-to-face ( $D_{3d}$ ) orientation, is illustrated in Figure 1. Three of the six bonds of each reactant molecule are ruptured, and a six-membered ring, reminiscent of chair cyclohexane, is formed to complete the cube.

The reaction can thus be discussed as if it involves only 12 electrons in six bonding orbitals, since the remaining 14 doubly occupied molecular orbitals retain their identity along the reaction path. Therefore, for the construction of the OCAMS correspondence diagram in Figure 2, we require two sets of six molecular orbitals; those on the left are linear combinations of the six bonding orbitals of the two  $P_4$  that are broken, and those on the right are LCBOs of the newly formed bond orbitals in  $P_8$ .

Five pairs of LCBOs are seen to be in direct correspondence across the diagram. The sixth pair is not, the nonmatching irreducible representations being  $a_{2u}$  on the left and  $a_{1u}$  on the right. By the rules of OCAMS,<sup>8</sup> a correspondence can be induced between these two orbitals by distorting the elongated cube along an  $a_{2g}$  ( $=a_{2u} \times a_{1u}$ ) symmetry coordinate, thereby reducing the symmetry along the reaction path to  $S_6$ , the subgroup of  $D_{3d}$  that is the kernel of  $a_{2g}$ .

However, as a conventional vibrational analysis<sup>9</sup> will confirm, the 18 internal symmetry coordinates of  $P_8$ —like its 18 normal modes—transform in  $D_{3d}$  as [ $3a_{1g} + a_{1u} + 2a_{2u} + 3e_g(2) + 3e_u(2)$ ]. There is no symmetry coordinate of the species,  $a_{2g}$ , such as would be required in order to “allow” the reaction. The dissociation reaction and its inverse, the dimerization of  $P_4$ , are thus both strictly “forbidden” at the molecular orbital level.

To be sure, a more drastic reduction of symmetry, for example the simultaneous displacement along an  $a_{1u}$  and an  $a_{2u}$  coordinate, would bring the two offending orbitals into correspondence, since both would have the same irreducible representation (a) in the ensuing subgroup of  $S_6$  ( $C_3$ ), but any such distortion would be opposed by a large restoring force. The same could be said about the still more drastic reduction of symmetry to  $C_i$ , in which both orbitals would map on to  $a_u$ . We therefore conclude that any pathway retaining  $D_{3d}$  symmetry will be blocked by a massive barrier which, moreover, cannot be circumvented by any reduction of symmetry that does not present excessive energetic demands.

### Semiempirical Pathway Computations (MNDO)

The  $P_8$  molecule has three independent geometric degrees of freedom in  $D_{3d}$ , as can be determined from a simple algorithm<sup>10</sup> or from the vibrational analysis just cited, which specifies—equivalently—that there are three totally symmetric normal modes.

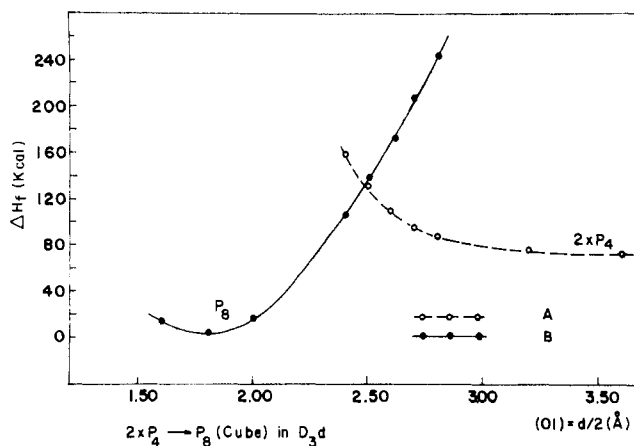


Figure 3. Attempted calculation of  $D_{3d}$  reaction path: (A) compression of the two  $P_4$ ; (B) stretching of  $P_8$ .

Half the length of the diagonal (01) was chosen to be the “reaction coordinate”; as it was varied, the other two independent parameters, chosen to be the length of the edge (12) and the angle between (01) and (12), were optimized. The result of two such calculations is shown in Figure 3. In the first, two separated  $P_4$  molecules are pushed together by decreasing (01); in the second,  $P_8$  is stretched by gradually increasing (01).

The curves in Figure 3 appear to cross at (01) = 2.475 Å, but they represent two distinct species, with different values of (12) and  $\angle 012$ . One, which we recognize to be “compressed two  $P_4$ ”, has the electronic configuration A( $[4a_{1g}^2, 4a_{2u}^2, 3e_g^4, 3e_u^4]$ ). The other, “stretched  $P_8$ ”, is B ( $[4a_{1g}^2, 1a_{1u}^2, 3a_{2u}^2, 3e_g^4, 3e_u^4]$ ). In agreement with Figure 2, the two configurations differ only with respect to the symmetry species of a single pair of occupied orbitals,  $a_{2u}$  in A and  $a_{1u}$  in B. This mismatch suffices to separate the two molecular species by a high ridge on the potential energy hypersurface.

A crossing from A to B can be forced by fixing (01) at 2.475 Å and varying (12) from 1.9 to 2.3 Å. A smooth transition is effected only when the minimal amount of configuration interaction available in the MNDO program is included. Its effect on the energy is small—only a few kilocalories—but it rescues the calculations from being discontinued on the grounds of being “unable to achieve self-consistency”.

A three-dimensional plot is shown in Figure 4. The energy maximum ( $\Delta H_f = 175$  kcal at (12) = 2.05 Å) lies more than 100 kcal above the two  $P_4$  and nearly 170 kcal above  $P_8$ . The region around this point was not explored thoroughly enough to characterize it firmly as “the transition state” for the reaction. However, the number of points that were calculated near it was sufficient to confirm the presence of a long energy ridge separating the two species. Moreover, reducing the symmetry to  $C_3$  or to  $C_i$ , the low-symmetry subgroups of  $D_{3d}$  in which  $a_{1u}$  and  $a_{2u}$  map onto the same irreducible representation, does not lower the energy near the barrier. One can be confident that distortion of the reacting system along a coordinate that reduces the symmetry to any of the other subgroups of  $D_{3d}$ , in which  $a_{1u}$  and  $a_{2u}$  map onto different irreducible representations, will be completely ineffective.

(9) See e.g.: Wilson, E. B., Jr.; Decius, J. C.; Cross, P. C. “Molecular Vibrations”; McGraw-Hill: New York, 1955; p 105 ff.

(10) Pople, J. A.; Sataty, Y. A.; Halevi, E. A. *Isr. J. Chem.* 1980, 19, 290.

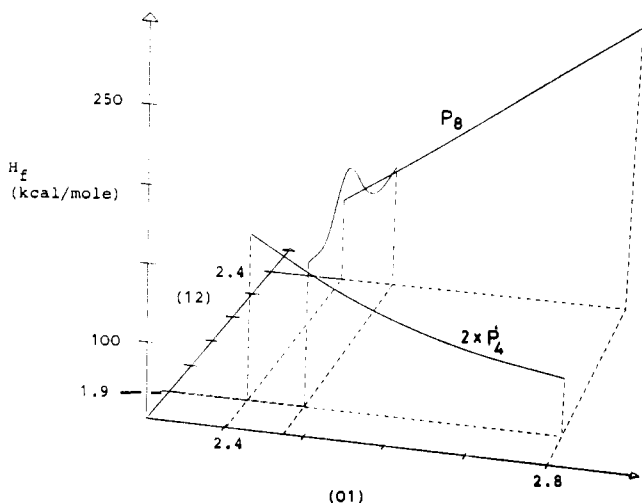


Figure 4. Crossing from A to B in  $D_{3d}$  at  $(01) = 2.475 \text{ \AA}$ .

### Conclusions

The presence of a barrier some 100 kcal high to the dimerization of tetrahedral  $P_4$  to cubic  $P_8$  has been established computationally. The calculations confirm the results of the orbital symmetry analysis, which predicts the presence of such a barrier, ascribing it to the incompatibility of one doubly occupied LCBO of the two  $P_4$  ( $a_{2u}$ ) with one of  $P_8$  ( $a_{1u}$ ), which cannot be overcome by any reduction of symmetry below  $D_{3d}$ , which is both geometrically feasible and energetically convenient.

An energy barrier of this magnitude should be sufficient to prevent the formation of cubic  $P_8$  at temperatures below that at which  $P_4$  is fully dissociated to  $P_2$ , particularly if routes to more stable species such as red  $(P_4)_n$  are available. The possible formation of noncubic  $P_8$  species, which can serve as possible intermediates in the polymerization process, is presently being explored.<sup>11</sup>

**Acknowledgment.** We are grateful for financial support (to E.A.H.) from the Minerva Foundation and The Fund for Promotion of Research at the Technion and (to H.B. and B.R.) from the Deutsche Forschungsgemeinschaft. We thank the Hochschul-Rechenzentrum of the Universität Frankfurt and the Technion Computer Center for making computer time available to us.

**Registry No.** Phosphorus, 7723-14-0.

(11) Bock, H.; Roth, B.; Hajevi, E. A. unpublished results.

Contribution from the Chemistry Departments, State University of New York, Albany, New York 12222, and State University of New York, Plattsburgh, New York 12901

### EPR of Copper(II) Complexes with Tripodal Ligands: Dynamical Properties

G. Kokoszka,<sup>\*1a</sup> K. D. Karlin,<sup>1b</sup> F. Padula,<sup>1a</sup> J. Baranowski,<sup>1a,c</sup> and C. Goldstein<sup>1a</sup>

Received January 23, 1984

A major theme in bioinorganic chemistry is the understanding of the role played by metal ions in metalloenzymes with particular focus on their unique characteristics. Many

(1) (a) State University of New York, Plattsburgh. (b) State University of New York, Albany. (c) Permanent address: Institute of Chemistry, Wrocław, Poland.

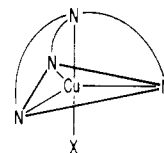


Figure 1.

of the iron proteins can be successfully modeled because they contain extrinsic active sites which may be reasonably reproduced outside of the actual protein. By contrast, copper proteins possess intrinsic active sites which are uniquely defined by the interactions of the ligating protein residues with the copper ions.<sup>2</sup> Thus, much of the activity in generating model systems for copper proteins has focused on small, well-defined structural or spectroscopic analogues that allow a particular feature(s) to be examined in detail. Many of the studies heretofore have examined the static spectral characteristics because these aspects may (or even must) be understood before additional dynamical features can be explored. Nevertheless, it is clear that a detailed understanding of the motional adjustments of the metalloprotein are needed to provide information on reaction rates and other dynamical properties.<sup>3</sup> Indeed, since changing structural properties are believed to be important in influencing the chemistry of real copper-containing enzymatic systems,<sup>4-7</sup> a further step in modeling enzyme active sites and reactivity should be to examine the possible roles of dynamical distortions in physically realistic model systems.

This paper provides a vehicle for examining dynamical behavior by EPR spectroscopy on trigonal-bipyramidal (TBP) systems of the type  $[\text{Cu}(\text{TMPA})\text{X}]\text{PF}_6$ ,  $\text{TMPA} = \text{tris}(2\text{-pyridylmethyl})\text{amine}$  and  $\text{X} = \text{Cl}^-$  and  $\text{N}_3^-$ , in frozen solutions and as a single crystal for  $\text{X} = \text{Cl}^-$ . The latter material has been characterized by X-ray crystallography<sup>8</sup> and has in-plane bonding very close to the  $120^\circ$  expected in the ideal TBP geometry.<sup>8</sup> A schematic drawing is shown in Figure 1. The usefulness of some tripod ligands in studying and modeling certain aspects of the coordination chemistry and structural properties of five-coordinate copper(I) and copper(II) complexes is well established.<sup>8-13</sup> Furthermore, the general features of many EPR spectra of five-coordinate  $\text{Cu}(\text{II})$  covering the full range from TBP to square pyramidal are also now reasonably well understood within the framework of the  $C_{2v}$  model.<sup>14</sup> Of course, the well-known tendency of the  $\text{Cu}(\text{II})$  ion to prefer a square-pyramidal geometry has greatly limited the number of examples that approach the trigonal-bipyramidal limit. Thus  $\text{Cu}(\text{II})$  complexes near this limit might be expected to exhibit a rhombic EPR pattern and some do. On

(2) Solomon, E. I.; Penfield, K. W.; Wilcox, D. E. *Struct. Bonding (Berlin)* **1983**, *53*, 1-57 and references cited therein.

(3) Gurd, F. R. N.; Rothgeb, T. M. *Adv. Protein Chem.* **1979**, *33*, 77-166.

(4) An example of this kind is the dramatic structural changes expected and observed at  $\text{Cu}(\text{I})$ - $\text{Cu}(\text{II})$  centers in redox-active copper metalloproteins.

(5) Gray, H. B.; Solomon, E. I. In "Copper Proteins"; Spiro, T. G., Ed.; Wiley: New York, 1981; pp 1-40. Solomon, E. I. *Ibid.* pp 41-108.

(6) Bacci, M. *Struct. Bonding (Berlin)* **1983**, *55*, 67.

(7) Karlin, K. D.; Zubieta, J., Eds. "Copper Coordination Chemistry: Biochemical and Inorganic Perspectives"; Adenine Press: Guilderland, NY, 1983.

(8) Karlin, K. D.; Hayes, J. C.; Juen, S.; Hutchinson, J.; Zubieta, J. *Inorg. Chem.* **1982**, *21*, 4106 and references cited therein.

(9) Padula, F.; Goldstein, C.; Orsini, J.; Kokoszka, G.; Karlin, K. D. *Inorg. Chim. Acta* **1983**, *79*, 198-199.

(10) Zubieta, J.; Karlin, K. D.; Hayes, J. C. In ref 5, pp 97-108.

(11) Sorrell, T. N.; Jameson, D. L. *Inorg. Chem.* **1982**, *21*, 1014.

(12) Addison, A. W.; Hendriks, H. M. J.; Reedijk, J.; Thompson, L. K. *Inorg. Chem.* **1981**, *20*, 103.

(13) Thompson, L. K.; Ball, R. G.; Trotter, J. *Can. J. Chem.* **1980**, *58*, 1566-1576.

(14) Bencini, A.; Bertini, I.; Gatteschi, D.; Scozzafava, A. *Inorg. Chem.* **1978**, *17*, 3194.